Journal of Inflammation Research

Dovepress
Taylor & Francis Group

Open Access Full Text Article

ORIGINAL RESEARCH

Distinct Immunological Features Compared to Lichen Planus and Oral Lichen Planus

Dong Min Lim[1], DoYeon Kim[2], Hye-Min Ju[3,4], Sung-Hee Jeong[3,4], Yun Hak Kim[5–7], Soo-Min Ok[3,4], Hae Ryoun Park[2,5,8]

[1]Interdisciplinary Program of Genomic Data Science, Pusan National University, Yangsan, 50612, Republic of Korea; [2]Department of Oral Pathology, School of Dentistry, Pusan National University, Yangsan, 50612, Republic of Korea; [3]Department of Oral Medicine, Dental and Life Science Institute, Pusan National University School of Dentistry, Yangsan, 50612, Republic of Korea; [4]Department of Oral Medicine, Dental Research Institute, Pusan National University Dental Hospital, Yangsan, 50612, Republic of Korea; [5]Periodontal Disease Signaling Network Research Center, School of Dentistry, Pusan National University, Yangsan, 50612, Republic of Korea; [6]Department of Anatomy, School of Medicine, Pusan National University, Yangsan, 50612, Republic of Korea; [7]Department of Biomedical Informatics, School of Medicine, Pusan National University, Yangsan, 50612, Republic of Korea; [8]Department of Periodontology and Dental Research Institute, Pusan National University Dental Hospital, Yangsan, 50612, Republic of Korea

Correspondence: Soo-Min Ok, Department of Oral Medicine, School of Dentistry, Pusan National University, 49 Pusandaehag-ro, Mulgeum-eup, Yangsan-si, Gyeongsangnam-do, 50612, Republic of Korea, Tel +82-55-360-5243, Fax +82-55-360-5234, Email oksoomin@pusan.ac.kr; Hae Ryoun Park, Department of Oral Pathology, School of Dentistry, Pusan National University, 49 Busandaehak-ro, Yangsan, 50612, Republic of Korea, Tel +82-51-510-8250, Fax +82-51-510-8249, Email parkhr@pusan.ac.kr

Purpose: Lichen planus (LP) and oral lichen planus (OLP) share clinical and histological similarities, yet their distinct immunopathological mechanisms make differentiation and management challenging. Clarifying these differences is essential for accurate diagnosis and treatment. This study aimed to investigate the systemic immune profile of OLP using single-cell transcriptomics, identifying distinct immune cell subsets and signaling pathways contributing to its chronic inflammatory state. Additionally, it sought to compare the inflammatory lesion microenvironments of OLP and LP by analyzing key immune pathways and cellular interactions.

Methods: Peripheral blood mononuclear cells (PBMCs) were obtained from 16 OLP patients and 5 healthy controls. Single-cell transcriptomic data from PBMCs and lesion tissues of OLP and LP were analyzed to profile immune and inflammatory signatures. Key molecular findings were validated using independent datasets and enzyme-linked immunosorbent assays (ELISA).

Results: Prostaglandin D2 synthase (*PTGDS*), a pivotal enzyme in prostaglandin metabolism, emerged as a diagnostic marker with elevated expression in NK cells from OLP patients. Additionally, a novel *CXCR4*^{high}–*TSC22D3*^{high} CD4 cytotoxic T cell subset with enhanced cytotoxicity was identified, potentially contributing to OLP pathogenesis. OLP blood samples also demonstrated significant upregulation of TNF and TLR signaling in NK cells, indicating a heightened chronic inflammatory state. Comparative tissue analysis revealed intensified TNF-driven inflammation and a disrupted *HIF1A*– vascular endothelial growth factor (VEGF) interactions in OLP, contrasting with LP's robust VEGF-mediated angiogenesis.

Discussion: These findings highlight distinct immunopathogenic mechanisms between OLP and LP. The upregulation of *PTGDS* in NK cells and *CXCR4*^{high}–*TSC22D3*^{high} CD4 cytotoxic T cells in PBMCs indicates systemic immune dysregulation in OLP, while tissue-level differences suggest impaired vascular remodeling and chronic inflammation. These insights underscore the need for targeted immunomodulatory therapies.

Conclusion: This study identifies distinct immune signatures that differentiate OLP from LP, highlighting potential therapeutic targets that require further validation for personalized treatment strategies.

Plain Language Summary: Lichen planus (LP) and oral lichen planus (OLP) are inflammatory conditions that affect the skin and mouth. Although they appear similar, our study shows that they are driven by different immune responses, which may require distinct treatment approaches. Understanding these differences can help doctors provide better care for each condition.

In this study, we analyzed blood and tissue samples from people with OLP and compared them to samples from healthy individuals and those with LP. We used tissue samples from healthy individuals undergoing orthognathic surgery as a control group. By studying gene activity at the level of individual cells, we identified a protein called *PTGDS* that was elevated in OLP, especially in a type of immune cell known as natural killer (NK) cells. *PTGDS* could serve as a valuable marker for diagnosing OLP.

Received: 26 November 2024
Accepted: 5 March 2025
Published: 18 March 2025

Graphical Abstract

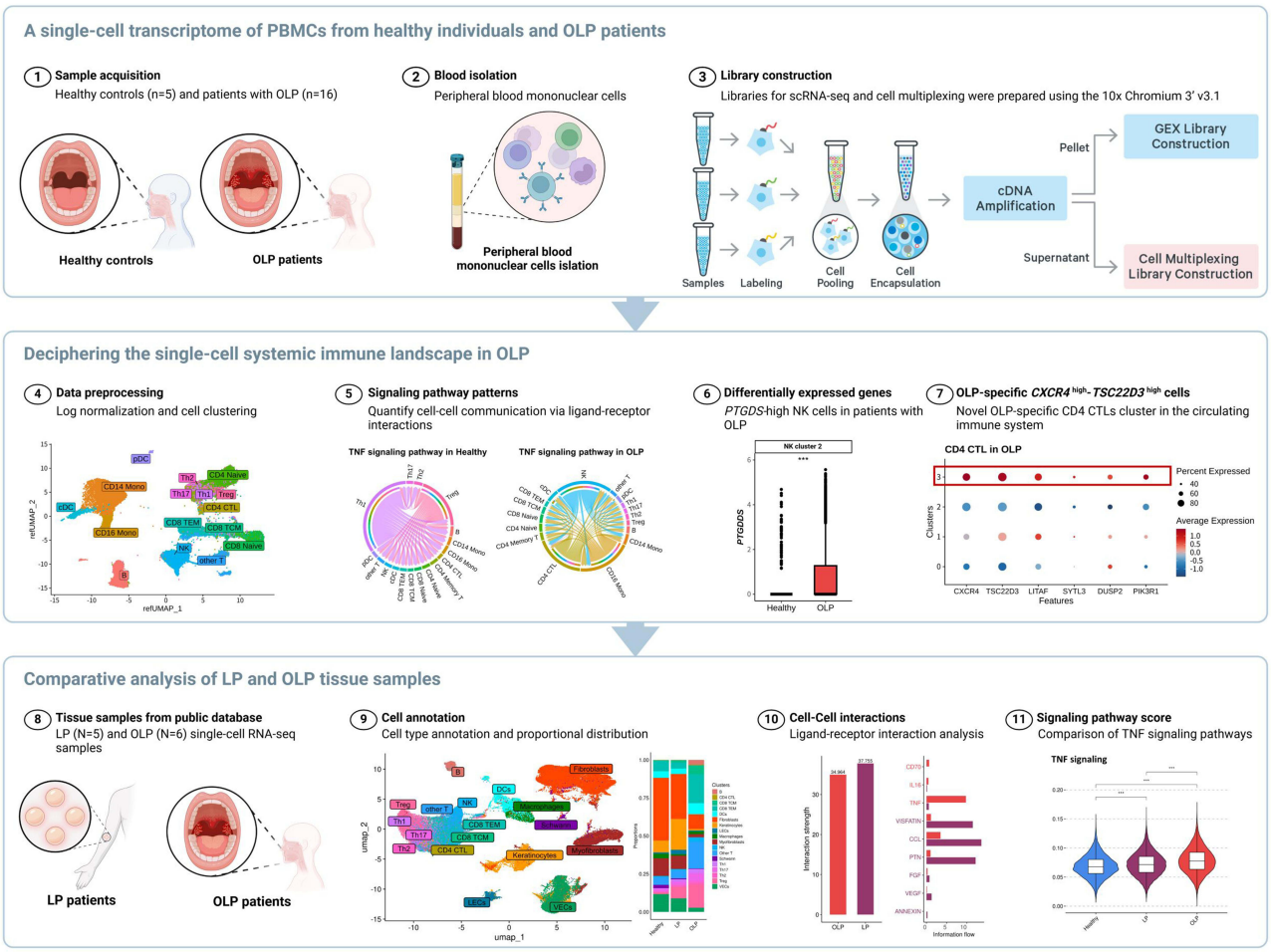

We also discovered a unique group of immune cells in OLP that exhibited increased activity, possibly contributing to ongoing inflammation. Additionally, OLP and LP displayed distinct microenvironments, with OLP samples showing higher activity in certain inflammation-related pathways, suggesting a more chronic and persistent immune response compared to LP.

These findings reveal important differences between LP and OLP, providing insights that may lead to more effective, targeted treatments for each condition. Understanding these unique immune responses may ultimately improve patient outcomes by guiding more personalized approaches to managing LP and OLP.

Keywords: single-cell RNA sequencing, lichen planus, oral lichen planus, chronic inflammation, systemic immunity

Introduction

Lichen planus (LP) is a relatively common immune-mediated disorder that primarily affects middle-aged individuals and can involve the oral mucosa, skin, and other mucosal surfaces. Oral lichen planus (OLP), a subset of LP, manifests as chronic lesions in the oral cavity, causing discomfort rather than extreme pain. Symptoms such as burning sensations, sensitivity to hot, acidic, or spicy foods, and irritation when brushing can significantly impair daily activities like speaking and chewing, leading to a reduced quality of life for OLP patients. These lesions tend to persist for many years, characterized by periods of exacerbation and remission, making OLP a chronic and intractable condition.[1,2] Though the

disease is not fatal and some lesions are even asymptomatic and thus no treatment is needed, it is notorious for its chronicity and intractability, especially in OLP. To develop effective treatment strategy against diseases, it is essential to understand its causative factors and its pathogenesis clearly, but the exact cause and its involved mechanism of OLP remains elusive. Stress, anxiety, mechanical trauma, hypersensitivity reactions, and viral infections have been suggested as contributing factors. However, studies have not confirmed a direct causal relationship, instead recognizing them as co-factors or triggers.[3–5] Though the correct cause in the development of OLP is controversial, it is evident that the pathogenesis is based on sophisticated immune reaction to a certain causative factor.

There is a consensus among researchers that the development of OLP begins with the recognition of irritants, triggering a complex interplay between various immune and non-immune cells, cytokines, and adhesion molecules.[6–9] This intricate process ultimately results in a dysregulated cell-mediated immune response. This immune response leads to the degradation of the basement membrane through proteolytic mechanisms and an inappropriate immune reaction, primarily orchestrated by specific T-cell subsets. These T-cells target oral keratinocytes, ultimately leading to the apoptosis of these cells as well. While T cells play important roles in the pathogenesis of OLP, their actions are influenced by various immune interactions.[9,10] Therefore, simply inhibiting or targeting them without a thorough understanding may not directly lead to safe and effective treatments.[11]

The recent advancements in single-cell transcriptomics provide a powerful tool with unprecedented resolution for dissecting complex immune ecosystems.[12–14] This has been instrumental in aiding the identification of inflammatory cell states, immune cell subsets, and functional states in the systemic immunity of chronic inflammatory diseases.[15–19] Using this technology, our study aimed to characterize the single-cell transcriptional atlas of peripheral blood mononuclear cells (PBMCs) in healthy controls and patients with OLP, providing discovery of diagnostic markers and novel insights into the immune landscape driving OLP pathogenesis in the context of systemic chronic inflammation.

While OLP and LP share some clinical and histological features, increasing evidence suggests that these two conditions are driven by distinct immunopathological mechanisms. These distinct immune and inflammatory pathways likely contribute to the differing clinical manifestations and disease progression of OLP and LP.[20] However, the specific immunopathological differences between OLP and LP remain poorly characterized, and a detailed investigation into these divergent pathways is critical for the development of targeted, disease-specific therapies.

Despite extensive research into the pathogenesis of OLP, including genetic, autoimmune, viral, and environmental factors, a comprehensive understanding of its immune landscape remains elusive. Clarifying this landscape is essential for advancing our knowledge of OLP and developing targeted immunomodulatory therapies that address systemic inflammation and improve patient outcomes. Additionally, understanding the distinct immunopathological differences and microenvironments of OLP and LP is essential for guiding clinical decision-making and developing more personalized treatments. By distinguishing their unique immune profiles, we can lay the foundation for tailored therapeutic approaches that target the specific inflammatory processes driving each condition.

Materials and Methods

Sample Acquisition

This study, approved by the Institutional Review Board of Pusan National University Dental Hospital, included 16 peripheral blood samples from OLP patients and 5 from healthy individuals. The blood samples were collected from the patients during the exacerbation period when their symptoms were severe, as they presented for their initial visit. OLP diagnosis was based on modified World Health Organization diagnostic criteria.[21] Table 1 outlines all clinical characteristics of the participants.

Single-Cell Preparation and Library Construction

Thawed cell stocks in 10% FBS/DMEM were washed and counted using a fluorescence cell counter. Cell viability was assessed using a dead cells removal kit. Cells were multiplexed with cell multiplexing oligos and pooled. Libraries for single-cell RNA-seq and cell multiplexing were prepared following the 10x chromium single-cell 3′ v3.1 protocol.

Table 1 Characteristics of Healthy Individuals and OLP Patients

Healthy			OLP		
Variable	**N**	**Mean (SD*)**	**Variable**	**N**	**Mean (SD*)**
Age (years)	5	43.6 (8.79)	**Age (years)**	16	51 (14.08)
	N	**Percentage (%)**		**N**	**Percentage (%)**
Sex	5		**Sex**	16	
Female	0	0	Female	11	68.75
Male	5	100	Male	5	31.25
Sample types			**Clinical classification**	16	
Blood	5	100	Reticular	1	6.25
			Erosive	5	31.25
			Ulcerative	7	43.75
			Unknown	3	18.75
			Sample types		
			Blood	16	100

Notes: *OLP, oral lichen planus; SD, standard deviation.

Abbreviations: CD4 CTLs, CD4 cytotoxic T lymphocytes; CD8 TCMs, CD8 central memory T cells; CD8 TEMs, CD8 effector memory T cells; cDCs, conventional dendritic cells; DEGs, differentially expressed genes; ELISA, enzyme-linked immunosorbent assay; FBS, fetal bovine serum; GO, Gene Ontology; HPCA, Human Primary Cell Atlas; KEGG, Kyoto Encyclopedia of Genes and Genomes; LAIR, leukocyte-associated immunoglobulin-like receptor; LP, lichen planus; NK cells, natural killer cells; OLP, oral lichen planus; PBMCs, peripheral blood mononuclear cells; PCA, principal component analysis; pDCs, dendritic cells; DCs, PGD2, prostaglandin D2; PGH2, prostaglandin H2; qPCR, quantitative polymerase chain reaction; RNA-seq, RNA sequencing; TCR, T-cell receptor; Th1, T-helper 1 cells; Th2, T-helper 2 cells; Th17, T-helper 17 cells; t-SNE, t-distributed Stochastic Neighbor Embedding; TLR, toll-like receptor; TNF, tumor necrosis factor; Tregs, regulatory T cells; UMAP, uniform manifold approximation and projection; UMIs, unique molecular identifiers; LR, ligand–receptor; VEGF, vascular endothelial growth factor; OSCC, oral squamous cell carcinoma.

Libraries were quantified using qPCR and sequenced on the HiSeq platform by Illumina, with approximately 20,000 read pairs per cell for gene expression and 5,000 read pairs per cell for cell multiplexing.

Single-Cell RNA-Seq and Data Processing

Quality and basic statistics of raw sequencing data were assessed with FastQC,[22] and data were processed using Cell Ranger v6.0.2 (10X Genomics) with the human genome (GRCh38).[23] Low-quality unique molecular identifiers (UMIs) were excluded, retaining cells with >500 and <6000 genes detected, and <5% mitochondrial reads. Data normalization was done via log transformation, identifying the top 2000 highly variable genes using variance-stabilizing transformation. Dimensionality reduction was performed, and data were annotated by mapping to a PBMC reference dataset with Seurat V4[24] and SingleR.[25]

Analysis of Single-Cell RNA-Seq Data

We followed a single-cell analysis pipeline that has been extensively validated in previously described studies.[12–14] The data were processed using the Seurat (v4.3.0).[24] Differentially expressed genes (DEGs) were identified using the "FindMarkers" function with the Wilcoxon test, defining DEGs by adjusted p-values < 0.05 and |logFC| > 0.25. Adjusted p-values were calculated using the Benjamini-Hochberg (BH) correction method. Cell type proportions were analyzed using the propeller R package[26], with statistical significance assessed via linear modeling after variance stabilization. Cell–cell interactions were explored using CellChat,[27] while gene signature scores were computed from Gene Ontology (GO) and Kyoto Encyclopedia of Genes and Genomes (KEGG) pathway gene sets using the UCELL package[28] and the Mann–Whitney U statistic. Specifically, we adapted the tumor necrosis factor (TNF) signaling pathway (hsa04668), Toll-like receptor (TLR) signaling pathway (hsa04620), apoptotic signaling pathway (GO:0097190), leukocyte migration (GO:0050900), T cell activation via T-cell receptor (TCR) (GO:0002291), immune tolerance (GO:0002507), 12 cytotoxicity-associated genes (*PRF1, IFNG, GNLY, NKG7, GZMB, GZMA, GZMH, KLRK1, KLRB1, KLRD1, CTSW*, and *CST7*), and 6 well-defined exhaustion markers (*LAG3, TIGIT, PDCD1, CTLA4, HAVCR2*, and *TOX*).[29]

Independent Validation Cohort

We obtained single-cell RNA sequencing data (accession number: HRA002370)[30] from patients with OLP, including both peripheral blood and tissue samples, through the National Genomics Data Center. For LP lesion tissue, we utilized single-cell RNA sequencing data from the NCBI Gene Expression Omnibus (GEO) database (accession number: GSE254542),[31] enabling a comparative analysis of immune and cellular dynamics between OLP and LP. Tissues from healthy individuals undergoing orthognathic surgery were used as controls. All participants, including patients and controls, had no history of prior treatment. The clinical characteristics of HRA002370 and GSE254542 are shown in Supplementary Tables 1 and 2, respectively.

Enzyme-Linked Immunosorbent Assay

PBMC samples from 23 healthy controls and 38 OLP patients were collected in EDTA vacutainers. Plasma was isolated by centrifugation and stored at −80°C. Protein levels were measured using an Enzyme-linked immunosorbent assay (ELISA) kit (MyBiosource, Cat. No. MBS160094) following the manufacturer's protocol, with absorbance read at 405 nm.

Statistical Analysis

Statistical analysis was conducted using R v4.1.3. Differences between groups were assessed with an unpaired Welch's *t*-test, and gene correlations were evaluated using the Spearman correlation coefficient. Significance was set at $p < 0.05$ (two-sided).

Results

A Single-Cell Transcriptional Atlas of PBMCs in Healthy Controls and OLP Patients

We conducted an integrated analysis of single-cell transcriptome data from healthy controls (n=5) and patients with OLP (n=16) to characterize the single-cell profiles of PBMCs. We then performed data preprocessing and quality control by filtering out low-quality UMIs, resulting in a total of 122,299 single cells being profiled (Healthy controls: 31,500 cells; OLP: 90,799 cells) (Figure 1A, and Supplementary Figure 1). We utilized Seurat v4[24] and singleR,[25] a reference-based mapping approach, to annotate the major cell types in PBMCs. In total, we identified 17 major cell types: B cells, CD14 Monocytes, CD16 Monocytes, CD4 cytotoxic T lymphocytes (CD4 CTLs), CD4 memory T cells, CD4 naive T cells, CD8 naive T cells, CD8 central memory T cells (CD8 TCMs), CD8 effector memory T cells (CD8 TEMs), conventional dendritic cells (cDCs), natural killer (NK) cells, other T cells, plasmacytoid dendritic cells (pDCs), T-helper (Th) 1 cells, Th2 cells, Th17 cells, and regulatory T cells (Tregs) (Figure 1B). To validate the accuracy of the reference-based annotation, we examined the expression patterns of marker genes for cell types using uniform manifold approximation and projection (UMAP) plots (Supplementary Figure 2). The cell percentages for each sample are provided in Supplementary Table 3. Of note, the proportions of Th17, Th2, and CD4 Memory T cells tended to be higher in OLP patients compared to the healthy controls (Figure 1C, and Supplementary Table 4). Then, we evaluated the cytotoxicity and exhaustion scores, which are considered significant in chronic inflammatory diseases, between OLP patients and healthy control group for each cell type. CD4 CTLs and NK cells exhibited higher cytotoxicity scores in OLP patients. Conversely, B cells, CD4 naive T cells, CD8 TEMs, and Th1 cells showed higher cytotoxicity scores in healthy controls. CD4 CTLs and NK cells also demonstrated higher exhaustion scores in OLP patients. Other T cells and Tregs exhibited higher exhaustion in OLP patients, too. In contrast, CD4 Memory T cells showed decreased exhaustion scores in OLP patients (Figure 1D and E). Previous studies have reported abnormal regulation of genes associated with TNF and TLR signaling in patients with OLP.[32,33] Therefore, we additionally compared the expression levels of gene sets related to TNF and TLR signaling pathways between OLP patients and healthy controls. Both TNF (OLP mean:10.53; healthy controls mean:10.31) and TLR (OLP mean: 6.73; healthy controls mean: 6.71) signaling scores showed higher expression levels in OLP patients (Figure 1F and G). In particular, TNF signaling was highly expressed in lymphoid cells within PBMCs of OLP patients compared to healthy controls. However, in the case of TLR, the increase was not as

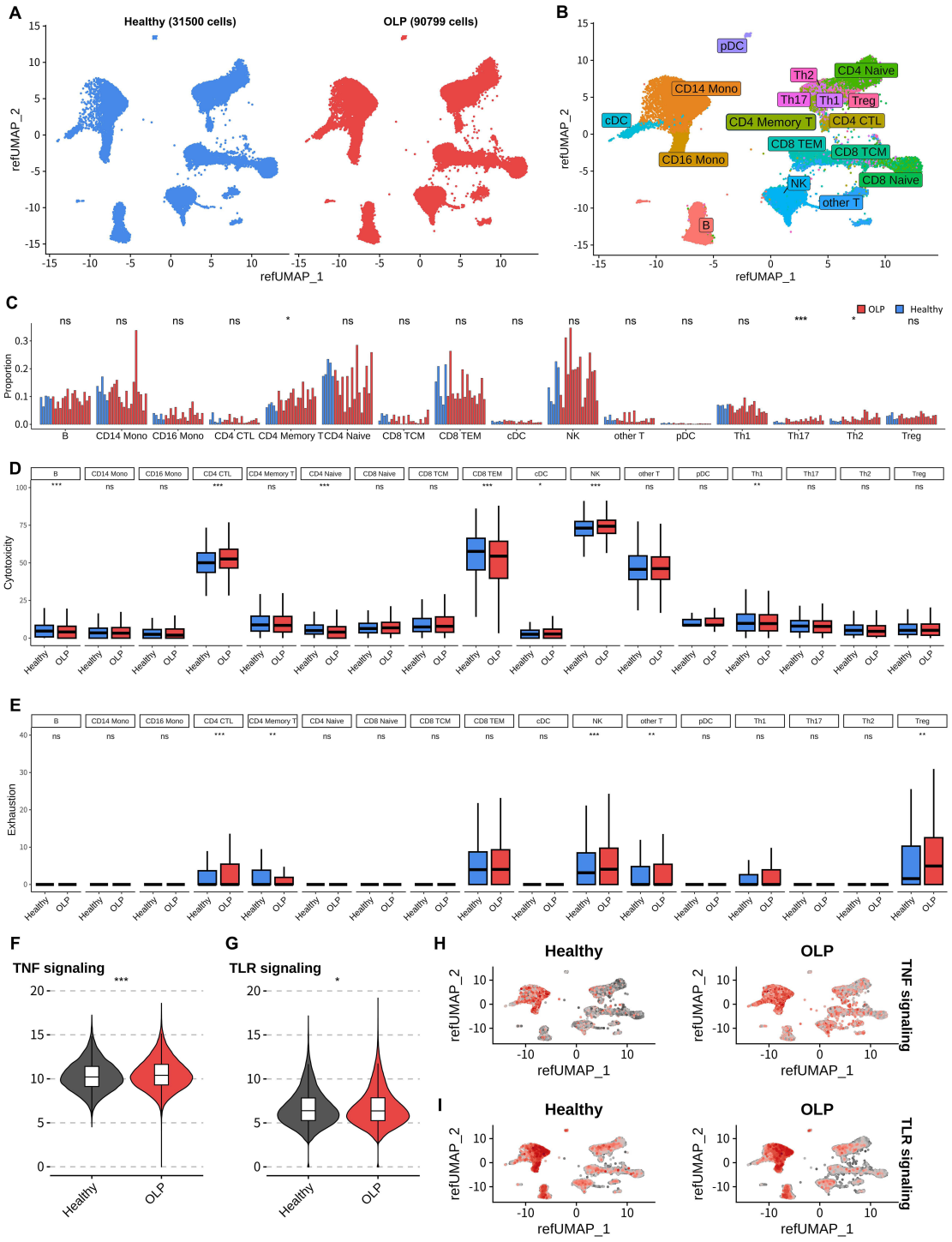

Figure 1 Single-cell transcriptional profiling of PBMCs from healthy controls and patients with OLP. (**A**) UMAP plot of cells from healthy and OLP samples. (**B**) UMAP plot showing annotated cell types identified through multi-modal reference mapping, with colors representing different cell types. (**C**) Bar graph showing cellular composition at the individual sample level. Statistical significance is indicated by asterisks (Welch's *t*-test). (**D**) Box plots of cytotoxicity gene set signature scores in healthy controls (n = 5) and OLP samples (n = 16). Groups are color-coded. Horizontal lines represent median values, with whiskers extending to 1.5 times the interquartile range. (**E**) Box plots of exhaustion gene set signature scores in healthy controls (n = 5) and OLP samples (n = 16). Groups are color-coded. Horizontal lines represent median values, with whiskers extending to 1.5 times the interquartile range. (**F**) Violin plot comparing TNF signaling gene set signature scores between healthy controls (n = 5) and OLP patients (n = 16), including a box plot. Horizontal lines represent median values, with whiskers extending to 1.5 times the interquartile range (Unpaired *t*-test with Welch's correction, $p < 0.001$). (**G**) Violin plot comparing TLR signaling gene set signature scores between healthy controls (n = 5) and OLP patients (n = 16), including a box plot. Horizontal lines represent median values, with whiskers extending to 1.5 times the interquartile range (Unpaired *t*-test with Welch's correction, $p < 0.05$). (**H**) UMAP plot showing TNF signaling expression in healthy controls and OLP patients. Increased expression is represented by a shift toward red. (**I**) UMAP plot showing TLR signaling expression in healthy controls and OLP patients. Increased expression is represented by a shift toward red. Statistical significance is indicated as follows: ns: $p \geq 0.05$, *: $p < 0.05$, **: $p < 0.01$, ***: $p < 0.001$.

pronounced as with TNF. In other words, specific cell type differences were not evident, but there was a slight increase across all cell types (Figure 1H and I).

NK Cells Induced TNF Signaling Interactions in OLP Patients

We compared the expression levels of gene sets involved in the TNF and TLR signaling pathways from the KEGG database between OLP patients and healthy controls. Subsequently, we calculated signaling signature scores in each sample and compared them with clinical features. We evaluated sub-signaling pathways, such as TNF-p38 signaling, extrinsic apoptotic pathway, TNF-IRF1 signaling pathway, chemotactic effects, TLR4-IRF3/7 signaling pathway, TLR1/2/4-NFKB signaling pathway, and promotion of Th17 cells differentiation for each sample. The genes associated with the TNF and TLR signaling pathways were predominantly upregulated in OLP patients. Simultaneously, OLP patients exhibited an increased promotion of Th17 cells differentiation (Figure 2A). These findings suggest the uncontrolled inflammatory state in patients with OLP.

Then, we employed the CellChat algorithm to analyze and quantify cell-cell communication via ligand–receptor (LR) interactions. As shown in Supplementary Figure 3, the relative flow level of TNF signaling was significantly higher in OLP patients. To address the question of whether specific cells induce inflammatory interactions through TNF signaling in OLP, we first investigated differential signaling pathways and the pattern of outgoing signaling across cell groups. Interestingly, TNF signaling exhibited different signaling patterns between healthy controls and OLP patients (Figure 2B). NK cells, along with CD4 CTLs and monocytes, robustly activated the TNF signaling pathway in patients with OLP. In healthy controls, it was indicated that Th1 cells and Tregs predominantly induce the TNF signaling pathway (Figure 2C and D).

Prostaglandin D2 Synthase-High NK Cells Indicate a Higher Proportion in Patients with OLP

We hypothesized that NK cells within PBMCs of OLP patients would exhibit distinct molecular characteristics compared to cells from healthy controls. We initially clustered the healthy control group and the OLP patient group separately using the Louvain algorithm after log normalization and principal component analysis (PCA). Subsequently, we visualized 11 NK clusters using t-distributed Stochastic Neighbor Embedding (t-SNE) (Figure 3A). Notably, we observed a significant difference in the proportions of NK cell sub-clusters 2 and 5 between OLP patients and the healthy control group. Specifically, NK cluster 2 exhibited a higher proportion in OLP patients (Figure 3B), whereas NK cluster 5 showed a higher proportion in healthy controls (Figure 3C). We then assessed the cytotoxicity and exhaustion scores of NK cells across two clusters exhibiting differences in proportions (Figure 3D and E). The mean values of cytotoxicity and exhaustion scores for NK cluster 2 in OLP patients are 74.73 and 5.47, respectively. In healthy controls, the mean values of cytotoxicity and exhaustion scores are 73.15 and 4.92, respectively. For NK cluster 5, the mean value of cytotoxicity and exhaustion scores were 74.57 and 4.57 in OLP patients, compared to 73.36 and 5.55 in healthy controls. Welch's *t*-test comparing the mean difference between groups showed statistically significantly higher cytotoxicity scores in clusters 2 and 5 among OLP patients. This suggests an overall elevated level of cytotoxicity in NK cells from OLP patients. Cluster 5 of NK cells also showed exhaustion in the healthy controls. Prostaglandin D2 synthase (*PTGDS)* is a glutathione-independent prostaglandin D synthase that catalyzes the conversion of prostaglandin H2 (PGH2) to prostaglandin D2 (PGD2).[34] Based on the analysis of DEGs for each cell type between patients with OLP and healthy controls (Supplementary Table 5), *PTGDS* demonstrated upregulation in NK cells among patients with OLP compared to healthy controls. Additionally, increased *PTGDS* expression was observed in NK cluster 2, which showed a higher proportion in patients with OLP (Figure 3F). Moreover, higher *PTGDS* expression was consistently observed in NK cells from OLP patients in the HRA002370 dataset (Figure 3G). To validate whether *PTGDS* secretion was increased in patients, we utilized ELISA to measure the protein levels in the serum. The elevation of *PTGDS* expression was further confirmed in the plasma of both OLP patients and healthy controls, with the OLP group exhibiting a higher *PTGDS* level compared to the healthy group (Figure 3H and Supplementary Table 6). The leukocyte-associated Ig-like receptor (LAIR) is a small family of ITIM-containing inhibitory receptors, belonging to the Ig superfamily. LAIR-2 is a secreted

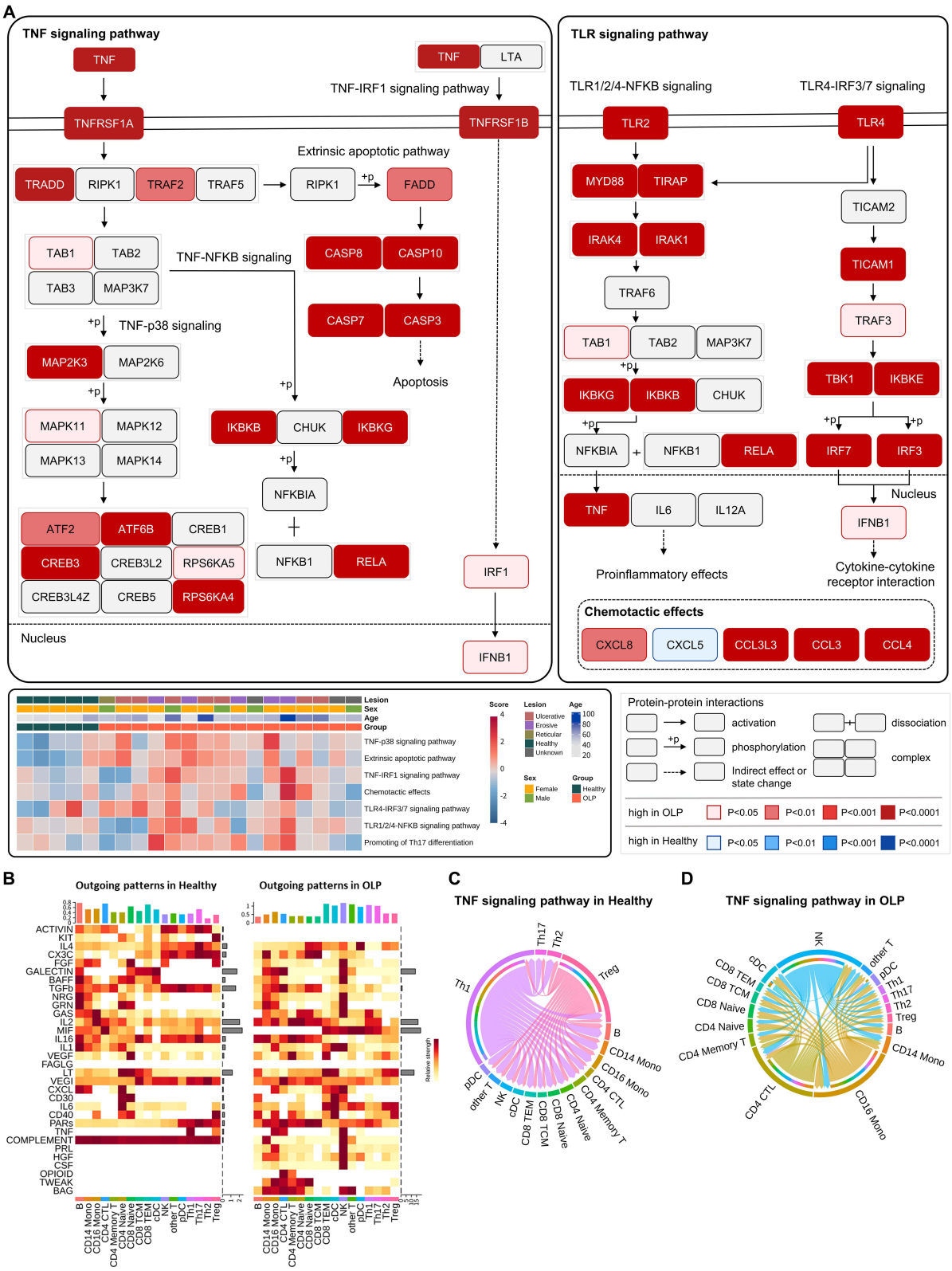

Figure 2 Cell-cell communication and signaling pathway. (**A**) Schematic diagram comparing gene expression levels of TNF and TLR signaling pathways between healthy controls and OLP patients. Solid lines represent the cell membrane; dotted lines represent the nuclear membrane. The diagram uses brightness to indicate statistical significance (based on an unpaired Welch's *t*-test), arrows for activation, bars for inhibition, and dotted arrows for indirect effects or state changes. The accompanying heatmap displays gene signature scores for pathways, with the top panel showing clinical characteristics (lesion, sex, and age). (**B**) Heatmap representing the relative signaling strength of an outgoing pathway across cell groups. The color bar indicates the overall signaling strength for each pathway, while the top colored bar plot shows the total signaling strength per cell group, and the right grey bar plot displays the total signaling strength per signaling pathway. (**C**) Chord plot illustrating TNF signaling pathway interactions in healthy controls. (**D**) Chord plot illustrating TNF signaling pathway interactions in OLP patients.

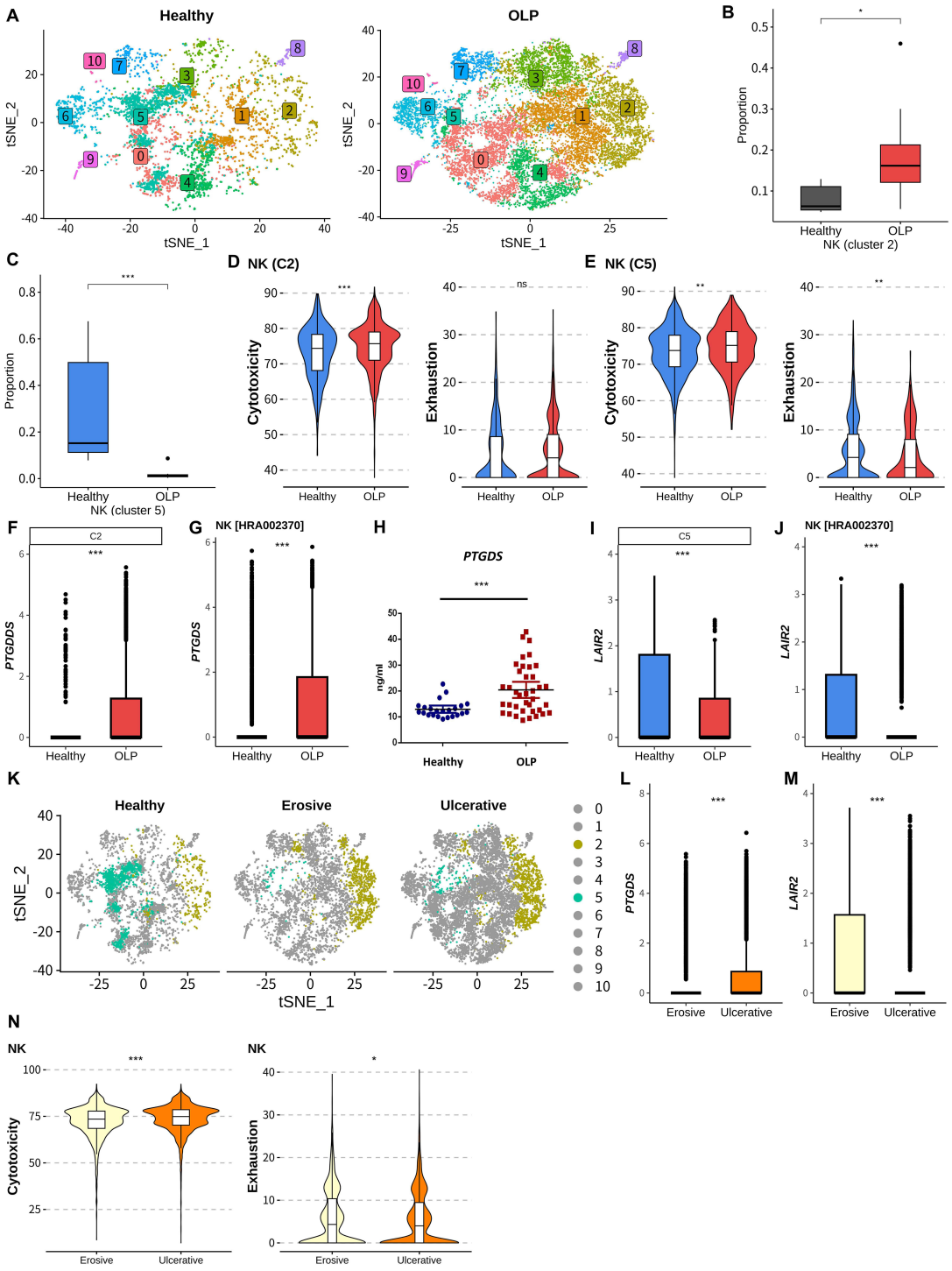

Figure 3 Characterization of NK cells in PBMCs of healthy controls and patients with OLP. (**A**) t-SNE plot of NK cells from healthy controls (left) and OLP patients (right). (**B**) Box plot of NK cluster 2 proportions (Unpaired *t* test with Welch's correction, $p < 0.05$). (**C**) Box plot of NK cluster 5 proportions (Unpaired *t* test with Welch's correction, $p < 0.001$). (**D**) Violin plot (with box plot overlay) comparing cytotoxicity ($p < 0.001$) and exhaustion scores ($p \geq 0.05$) in NK cluster 2 (Unpaired *t* test with Welch's correction). (**E**) Violin plot (with box plot overlay) comparing cytotoxicity ($p < 0.01$) and exhaustion scores ($p < 0.01$) in NK cluster 5 (Unpaired *t* test with Welch's correction). (**F**) Box plot of PTGDS expression in NK cluster 2 (Unpaired *t* test with Welch's correction, $p < 0.001$). (**G**) Box plot of PTGDS expression in NK cells validated with the HRA002370 dataset (Unpaired *t* test with Welch's correction, $p < 0.001$). (**H**) ELISA of plasma PTGDS levels in healthy controls (n = 23) and OLP patients (n = 38) (Unpaired *t* test with Welch's correction, $p < 0.001$). (**I**) Box plot of LAIR2 expression in NK cluster 5 (Unpaired *t* test with Welch's correction, $p < 0.001$). (**J**) Box plot of LAIR2 expression in NK cells validated with the HRA002370 dataset (Unpaired *t* test with Welch's correction, $p < 0.001$). (**K**) t-SNE plot of NK cells with OLP patients subdivided into erosive and ulcerative groups; NK clusters 2 and 5 are shown in different colors. (**L**) Box plot comparing PTGDS expression between erosive and ulcerative OLP lesions (Unpaired *t* test with Welch's correction, $p < 0.001$). (**M**) Box plot comparing LAIR2 expression between erosive and ulcerative OLP lesions (Unpaired *t* test with Welch's correction, $p < 0.001$). (**N**) Violin plot (with box plot overlay) comparing cytotoxicity ($p < 0.001$) and exhaustion scores ($p < 0.05$) between erosive and ulcerative OLP lesions (Unpaired *t* test with Welch's correction). Statistical significance is indicated as follows: ns: $p \geq 0.05$, *: $p < 0.05$, **: $p < 0.01$, ***: $p < 0.001$.

https://doi.org/10.2147/JIR.S506313

molecule, whereas LAIR-1 is its membrane-bound homologue. LAIR-2 is believed to play a regulatory role in the interaction between collagen and LAIR-1. It was identified due to its similarity to LAIR-1, a membrane-bound receptor that modulates the innate immune response.[35–37] *LAIR2* exhibited decreased expression in cluster 5 of NK cells in OLP patients (Figure 3I). Similarly, in the HRA002370 dataset, *LAIR2* was also validated to show decreased expression in OLP patients (Figure 3J). We evaluated the characteristics of NK cells based on the lesions of OLP patients, distinguishing between erosive and ulcerative. Clusters 2 and 5 of NK cells exhibited similar distributions in both erosive and ulcerative lesions (Figure 3K). A noteworthy observation is that OLP patients with ulcerative lesions showed higher *PTGDS* expression compared to patients with erosive lesions, while conversely, *LAIR2* exhibited decreased expression in ulcerative lesions (Figure 3L and M). Ulcerative lesions, which represent more severe and deeper tissue damage compared to erosive lesions, exhibited increased cytotoxicity, and decreased exhaustion levels (Figure 3N).

Features of T Cell Subsets in Patients with OLP

OLP is a chronic inflammatory oral mucosal disease of unknown etiology mediated by T cells.[38] We hypothesized that subsets of T cells within the PBMCs of OLP patients would exhibit distinct molecular characteristics compared to cells from healthy controls. We separated the data into 11 subsets of T cells. There were no significant differences in the subset proportions of T cells between erosive and ulcerative lesions compared to healthy controls (Figure 4A and B). We observed that DEGs upregulated in patients with OLP were involved in processes including cytokine production, cell migration, positive regulation of leukocyte cell-cell adhesion, and positive regulation of leukocyte-mediated cytotoxicity (Supplementary Table 7). In addition, using an apoptosis and migration scoring system, we observed that T cells in OLP patients likely underwent migration and apoptosis (Figure 4C and D). In patients with OLP, most subsets of T cells, including CD4 CTLs, CD4 Memory T, and Tregs, exhibited higher apoptosis and migration scores. The significant activation of apoptosis and migration pathways in T cells within the PBMCs of OLP patients may indicate an association between cell apoptosis and lymphocyte migration and the imbalance of the systemic immune system in OLP patients. Additionally, we compared the apoptosis (Figure 4E), migration (Figure 4F), T cell activation via T cell receptor (TCR) (Figure 4G), immune tolerance (Figure 4H), cytotoxicity (Figure 4I), and exhaustion (Figure 4J) scores of T cells in OLP patients to those in healthy controls based on the lesion type OLP is an inflammatory condition with autoimmune features. T cells from erosive and ulcerative patients exhibited lower immune tolerance scores compared to healthy controls (Figure 4H). These findings are consistent with previous studies suggesting that some patients with OLP may develop an autoimmune state attacking other target organs. Recent research has shown the coexistence of autoimmune thyroid disease and OLP, as well as type 1 diabetes and OLP. The association of OLP with other autoimmune processes implies the potential for OLP-affected patients to develop autoimmune states that actually trigger auto-aggression against other targets.[39,40]

CXCR4^{high}-TSC22D3^{high} CD4 CTLs Exhibit Increased Cytotoxicity in OLP Patients

We hypothesized that CD4 CTLs within the PBMCs of OLP patients would exhibit distinct molecular characteristics related to cytotoxicity compared to healthy controls. To address this question, we investigated genes co-expressed highly in CD4 CTLs from OLP patients and examined the characteristics of the CD4 CTLs clusters. As a result, we discovered a novel cell type showing independent features in OLP. A significant discovery is that both *CXCR4* and *TSC22D3* exhibited high expression in OLP patients in both our cohort and the HRA002370 dataset (Figure 5A and B). We also confirmed that *CXCR4* and *TSC22D3* were co-expressed with each other (Figure 5C and D). We divided the samples into high-expressed and low-expressed groups based on the mean values of *CXCR4* and *TSC22D3* expression levels, and additionally compared the percentage of cells expressing high levels of *CXCR4* and *TSC22D3* between patients with lesions and healthy controls *CXCR4*^{high}-*TSC22D3*^{high} CD4 CTLs showed the least distribution in healthy controls and the highest proportion in ulcerative lesions. *CXCR4*^{high}-*TSC22D3*^{high} CD4 CTLs showed the least distribution in healthy controls, and increased from erosive to ulcerative lesions (Figure 5E). This was also observed in the HRA002370 dataset, with OLP patients showing a higher proportion of *CXCR4*^{high}-*TSC22D3*^{high} cells within CD4 CTLs (Figure 5F).

To identify the existence of specific clusters with high expression of *CXCR4* and *TSC22D3*, we performed re-clustering of CD4 CTLs along with using the Louvain algorithm after log normalization and PCA. The significant finding is that CD4 CTLs cluster 3 exhibited notably high expression of *CXCR4* and *TSC22D3* in OLP patients, and we identified

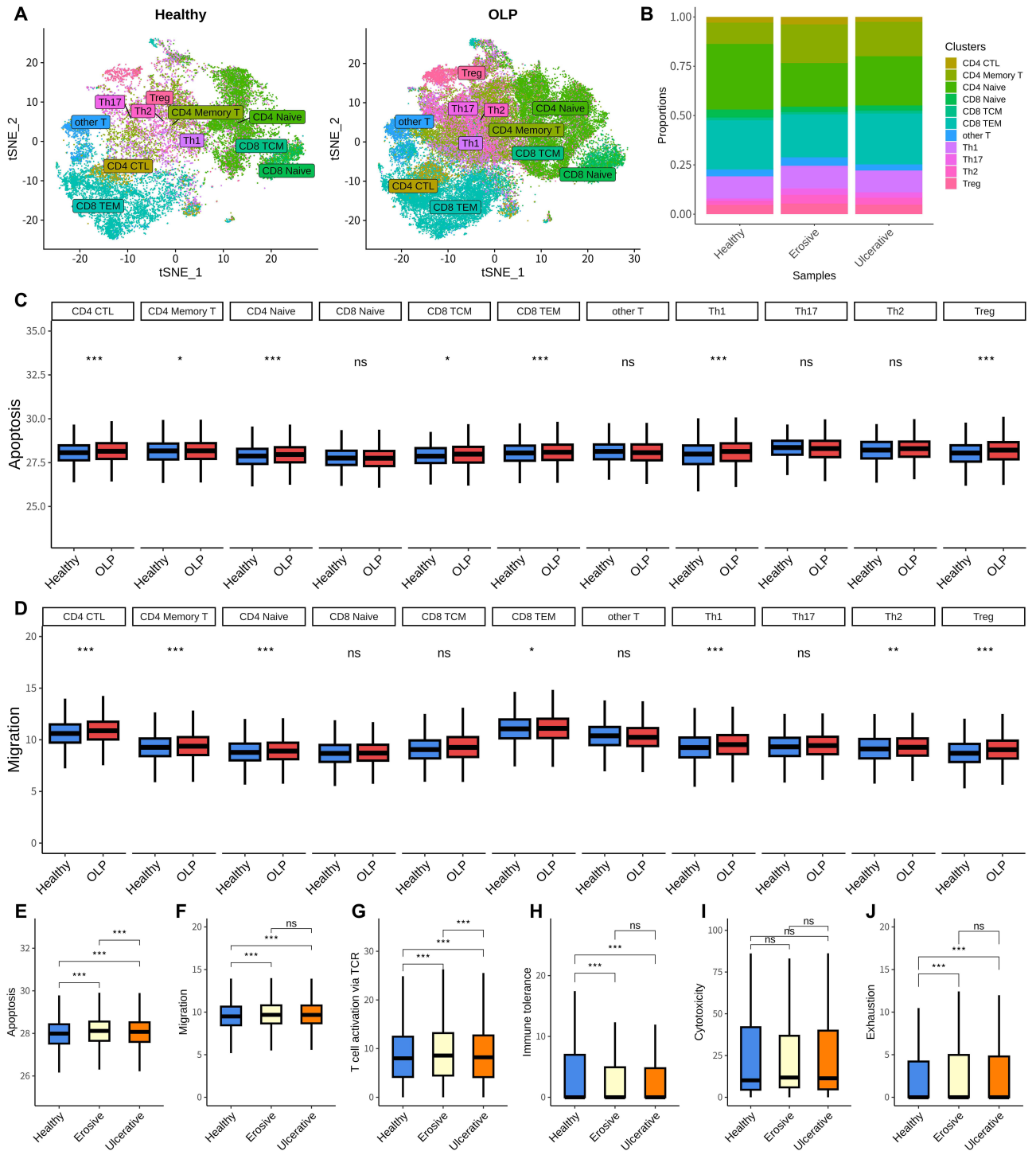

Figure 4 Characterization of T cell subsets in PBMCs of healthy controls and patients with OLP. (**A**) t-SNE plot of T cells; healthy controls (left) and OLP patients (right). (**B**) Bar plot of cell compositions in healthy controls and OLP patients, with OLP subdivided into erosive and ulcerative groups based on lesion type. (**C**) Box plots of apoptosis gene set signature scores in T cells from healthy controls (n = 5) and OLP patients (n = 16). Horizontal lines indicate median values; whiskers extend to 1.5 times the interquartile range. Statistical significance is indicated by asterisks (Welch's *t*-test). **D**) Box plots of T cell migration gene set signature scores in T cells from healthy controls (n = 5) and OLP patients (n = 16). Horizontal lines indicate median values; whiskers extend to 1.5 times the interquartile range. Statistical significance is indicated by asterisks (Welch's *t*-test). Box plots comparing gene set signature scores for apoptosis (**E**), migration (**F**), T cell activation via TCR (**G**), immune tolerance (**H**), cytotoxicity (**I**), and exhaustion (**J**) between healthy controls and OLP patients, stratified by lesion type (erosive vs ulcerative). Horizontal lines indicate median values; whiskers extend to 1.5 times the interquartile range. Statistical significance is indicated by asterisks (Welch's *t*-test). Statistical significance is indicated as follows: ns: $p \geq 0.05$, *: $p < 0.05$, **: $p < 0.01$, ***: $p < 0.001$.

https://doi.org/10.2147/JIR.S506313

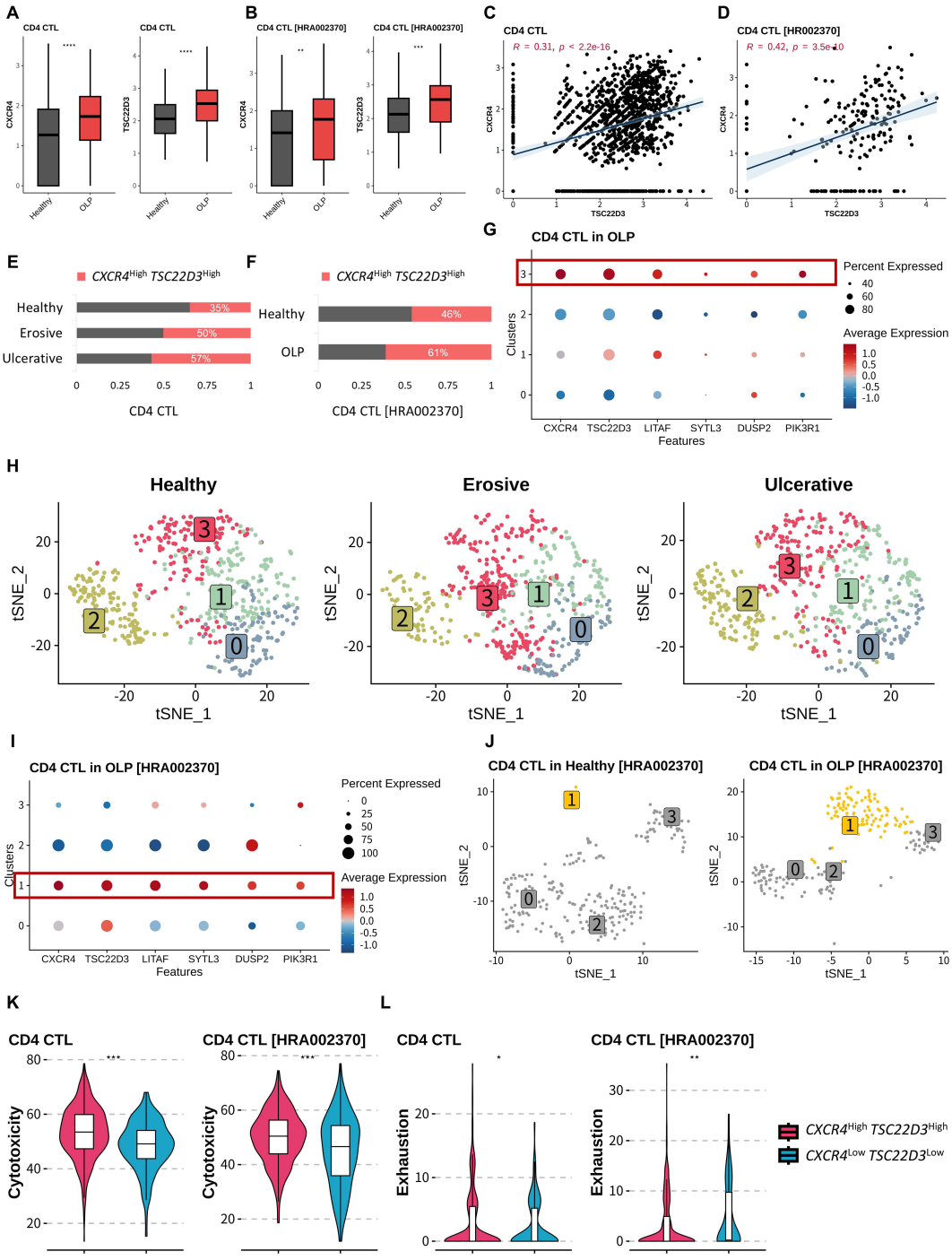

Figure 5 Classification of *CXCR4*^{high} *TSC22D3*^{high} CD4 CTLs in patients with OLP. (**A**) A box plot comparing the expression levels of *CXCR4* ($p < 0.001$) and *TSC22D3* ($p < 0.001$) in CD4 CTLs between healthy controls and OLP patients (Unpaired *t*-test with Welch's correction). (**B**) A box plot comparing the expression levels of *CXCR4* ($p < 0.001$) and *TSC22D3* ($p < 0.001$) in CD4 CTLs between healthy controls and OLP patients for validation using the HRA002370 dataset (Unpaired *t*-test with Welch's correction). (**C**) A Spearman correlation scatter plot shows a positive correlation between the expression levels of *CXCR4* and *TSC22D3* in CD4 CTLs of OLP patients. (**D**) A Spearman correlation scatter plot shows a positive correlation between the expression levels of *CXCR4* and *TSC22D3* in CD4 CTLs of OLP patients in the HRA002370 validation set. (**E**) The bar graph illustrates the cellular composition of CD4 CTLs with high *CXCR4* and high *TSC22D3* in healthy controls, erosive, and ulcerative groups. (**F**) Bar graph illustrating the cellular composition of *CXCR4*^{high} - *TSC22D3*^{high} CD4 CTLs in healthy controls and OLP patients from the HRA002370 dataset. (**G**) Dot plot displaying the expression levels of *CXCR4, TSC22D3, LITAF, SYTL3, DUSP2*, and *PIK3R1* in CD4 CTL clusters of OLP patients. (**H**) t-SNE plot displaying clusters within the CD4 CTL population of healthy controls, erosive, and ulcerative groups. (**I**) The dot plot illustrates the expression levels of *CXCR4, TSC22D3, LITAF, SYTL3, DUSP2*, and *PIK3R1* in CD4 CTLs clusters in patients with OLP from the HRA002370 dataset. (**J**) The t-SNE plot highlights cluster 1 within CD4 CTLs cells from the HRA002370 dataset. Healthy controls are displayed on the left, while OLP patients are shown on the right. (**K**) Violin plot comparing cytotoxicity scores between the *CXCR4*^{high} - *TSC22D3*^{high} and *CXCR4*^{low} - *TSC22D3*^{low} groups in CD4 CTL cells of OLP patients within our cohort and the HRA002370 validation set. (**L**) Violin plot comparing exhaustion scores between the CXCR4^{high} - TSC22D3^{high} and *CXCR4*^{low} - *TSC22D3*^{low} groups in CD4 CTL cells of OLP patients within our cohort and the HRA002370 validation set. Statistical significance is indicated as follows: ns: $p \geq 0.05$, *: $p < 0.05$, **: $p < 0.01$, ***: $p < 0.001$.

LITAF, SYTL3, DUSP2, and *PIK3R1* as marker genes for cluster 3 of CD4 CTLs (Figure 5G and H). Consistently, we identified cluster 1 of CD4 CTLs with high *CXCR4* and *TSC22D3* expression in the HRA002370 validation set, where it was predominant in OLP patients and showed similar marker gene characteristics (Figure 5I and J). Based on these results, we hypothesized that *CXCR4*^{high}-*TSC22D3*^{high} CD4 CTLs might also influence cytotoxic function. To answer this hypothesis, we evaluated cytotoxicity and exhaustion score systems. Ultimately, *CXCR4*^{high}-*TSC22D3*^{high} cells exhibited higher cytotoxicity and exhaustion compared to *CXCR4*^{low}-*TSC22D3*^{low} cells (Figure 5K and L). These findings highlight transcriptional features of CD4 CTLs in the blood of OLP patients, characterized by the disease's hallmark mediated by T cells, emphasizing the discovery of novel OLP-specific CD4 CTLs cluster in the circulating immune system.

Differential Microenvironment in OLP and LP Lesions

Single-cell transcriptomic analysis revealed distinct cellular subpopulations within tissue samples (Healthy controls:13190 cells; LP: 57036 cells; OLP: 30728 cells). UMAP projection (Figure 6A) and proportional composition (Figure 6B) illustrate these clusters. Specifically, fibroblasts (*COL1A1*), keratinocytes (*FLG, KRT14*, and *KRT1*), vascular endothelial cells (VECs) (*ENG*), lymphatic endothelial cells (LECs) (*CCL21*), myofibroblasts (*ACTA2* and *TAGLN*), lymphocytes (*CD3D* and *PTPRC*), Schwann cells (*SOX10*), B cells (*MS4A1*), dendritic cells (DCs) (*CLEC4C* and *XCR1*), and macrophages (*CD68*) were identified (Supplementary Figure 4). Immune cell subsets were annotated using the SingleR[25] reference-based algorithm. The relative distribution of T-cell subsets differed significantly among healthy controls, LP, and OLP samples, with OLP exhibiting a markedly higher proportion of CD8 TCMs, CD8 TEMs, and other T cells compared to the other groups (Figure 6C). To characterize differences in signaling networks within the lesion microenvironment of OLP and LP, we analyzed LR interactions, revealing distinct intercellular communication patterns between the two conditions. The overall interaction strength differed between the two conditions, with LP (37,755) exhibiting a higher total interaction strength compared to OLP (34,964) (Figure 6D). The analysis of LR interactions revealed significant differences in signaling pathways between OLP and LP (Figure 6E). Several key pathways exhibited distinct activation patterns, suggesting differential intercellular communication dynamics in the two conditions. Notably, CD70, IL16, and TNF signaling showed higher activity in OLP, whereas visfatin, C-C motif chemokine ligand (CCL), pleiotrophin (PTN), fibroblast growth factor (FGF), vascular endothelial growth factor (VEGF), and annexin signaling were more pronounced in LP. These findings indicate that the signaling environment within the lesion microenvironment is uniquely modulated in each condition, potentially contributing to their distinct pathophysiological characteristics. Notably, TNF signaling was significantly elevated in OLP lesions, consistent with its increased expression in PBMCs from OLP patients, indicating a systemic pro-inflammatory state. Moreover, intercellular communication within the TNF signaling pathway was more extensively activated in OLP than in LP, spanning a broad range of cell types (Figure 6F). This heightened TNF signaling was observed not only in $CD4^+$ and $CD8^+$ T-cell subsets but also in other lymphocytes, endothelial cells, and stromal cells in OLP. The widespread activation of *TNF* across these diverse cell populations suggests that OLP is characterized by an intensified inflammatory microenvironment, potentially driving disease progression through sustained *TNF*-mediated immune responses. These findings underscore the pivotal role of TNF signaling in shaping the inflammatory landscape of OLP, distinguishing it from the signaling dynamics observed in LP. TNF signaling was most strongly activated in OLP, as evidenced by both LR interactions and overall signaling scores. *TNF–TNFRSF1B* interaction showed strong activation specifically in OLP (Figure 6G). Additionally, TNF signaling scores exhibited a stepwise increase, with LP showing significantly higher scores than healthy controls, and OLP displaying a significantly greater TNF signaling score compared to LP (Figure 6H). While OLP exhibited a dominant *TNF*-driven inflammatory response, it also showed downregulated VEGF signaling, distinguishing its microenvironment from that of LP. VEGF-mediated intercellular communication was significantly weaker in OLP (Figure 6I) than in LP (Figure 6J), suggesting a limited pro-angiogenic response within OLP lesions. The reduced VEGF signaling in OLP, despite persistent inflammation, indicates a fundamentally distinct tissue remodeling process compared to LP. Interestingly, although *HIF1A*, a key hypoxia-related gene, was upregulated in OLP, VEGF LR interactions remained notably weaker in this condition. In contrast, LP exhibited both higher VEGF LR expression and stronger receptor engagement, supporting active angiogenesis (Figure 6K). These findings suggest that while hypoxia-associated signaling

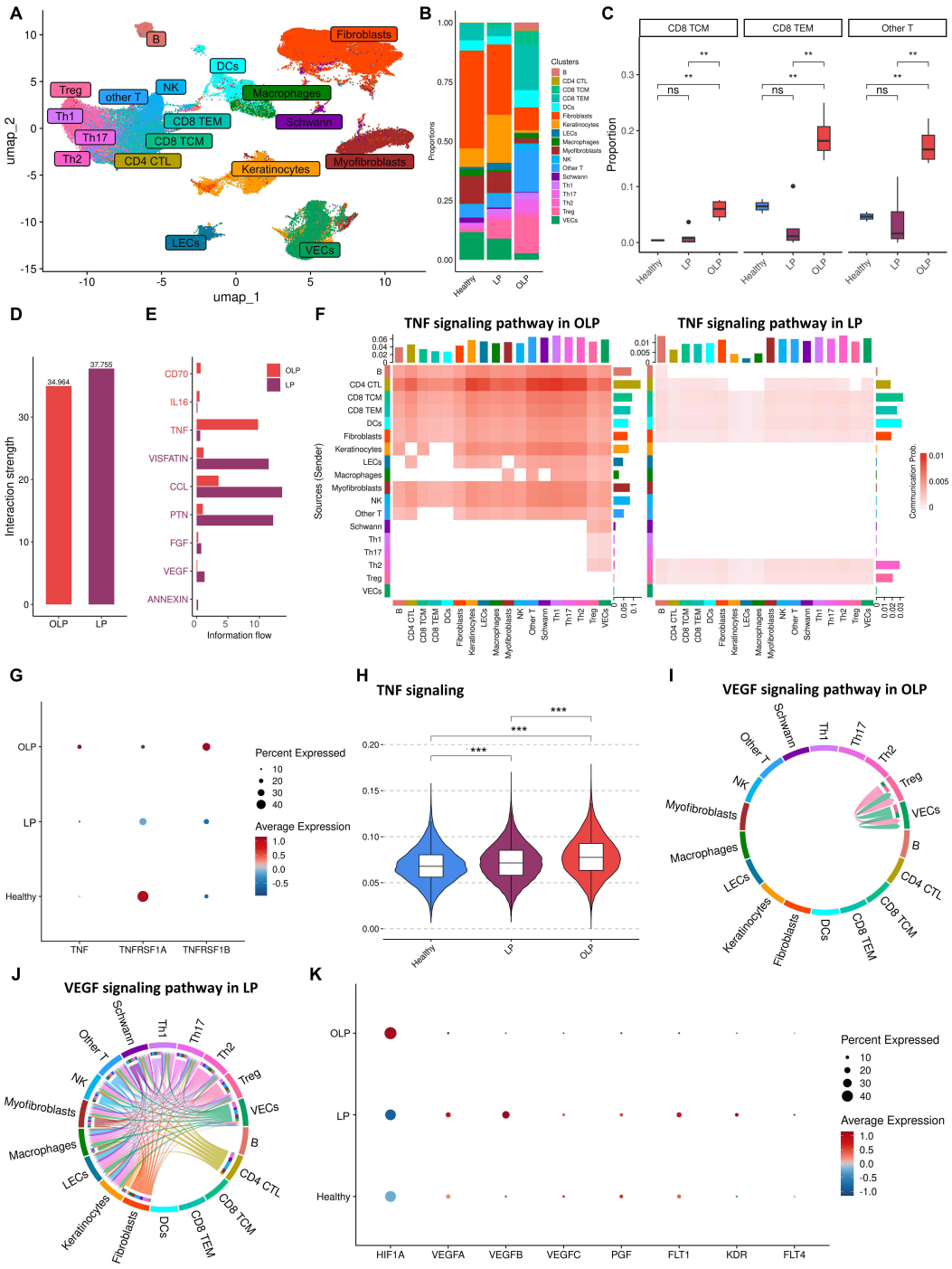

Figure 6 Comparative analysis of the microenvironment in OLP and LP. (**A**) A UMAP projection illustrating the subcluster distribution of single cells isolated from tissue samples. Each point represents a single cell, with its color and label indicating the assigned cell type. (**B**) A stacked bar chart illustrating the proportional distribution of each cellular subcluster across the groups. The vertical axis depicts the fraction of the total cell population, while the horizontal axis denotes the groups. (**C**) Box plots illustrating the relative distribution of specific T-cell subsets (CD8 TCMs, CD8 TEMs, and Other T cells) across the three groups (Healthy, OLP, and LP). The vertical axis indicates the percentage of each subset, and asterisks denote statistically significant differences (p-values). (**D**) A bar chart illustrating the comparative strengths of cell–cell interactions in both OLP and LP samples. (**E**) A bar chart comparing significant LR signaling pathways in OLP versus LP. (**F**) Heatmaps illustrate TNF signaling pathway activity across various cell types in OLP (left) and LP (right). The horizontal axis indicates the receiver cells, the vertical axis represents the sender cells, and the color scale bar reflects the signaling intensity. (**G**) Dot plot illustrating the expression of TNF signaling components across each groups. The dot size indicates the proportion of cells expressing each gene, while the color scale represents the corresponding expression level. (**H**) Violin plots compare overall TNF signaling scores across groups. Horizontal lines within the violins indicate median expression, and asterisks indicate statistical significance. (**I**) Chord diagram illustrating VEGF signaling interactions among different cell types in OLP. The thickness of each connecting chord indicates the magnitude of intercellular communication. (**J**) Chord diagram highlighting VEGF pathway connections in LP samples. (**K**) Dot plot illustrating the expression of *HIF1A* and the LR components of the VEGF signaling pathway across the three groups. The size of each dot represents the percentage of cells expressing each gene, and the color indicates the average expression level. Statistical significance is indicated as follows: ns: $p \geq 0.05$, **: $p < 0.01$, ***: $p < 0.001$.

is activated in OLP lesion, it does not effectively induce VEGF-mediated vascular remodeling, unlike in LP, where VEGF signaling is fully engaged.

Discussion

OLP is a T cell-mediated chronic inflammatory disorder that causes oral mucosal damage and pain. Although OLP and cutaneous LP share clinical and histological traits, emerging evidence suggests they are driven by distinct immunopathological mechanisms, leading to differences in clinical presentation and disease progression. However, these specific distinctions remain underexplored, hindering the development of targeted therapies.[41–43] Our study addresses this gap by providing a comprehensive single-cell analysis of the immune cell landscape in OLP, revealing key immune contributors to its pathogenesis. This work aims to advance clinical care and support the development of more personalized treatment strategies.

Our analysis identified a dysregulated immune response characterized by elevated proportions of specific T cell subsets, including Th17 cells, Th2 cells, and CD4 memory T cells, in OLP patients compared to healthy controls. Consistently, recent research has reported that Th17 and Th2 cells, along with their signature cytokines, play pivotal roles in the pathogenesis of OLP as well as autoimmune diseases.[44,45] These findings corroborate previous research implicating T cell-mediated immunity in OLP pathogenesis and highlight the role of cellular immunity in driving disease progression.[46] Furthermore, assessment of cytotoxicity and exhaustion scores unveiled heightened immune activity, particularly in CD4 CTLs and NK cells in OLP patients. The increased cytotoxicity and exhaustion levels suggest a state of chronic inflammation and immune dysregulation within the OLP microenvironment, which may contribute to disease pathogenesis and progression. Analysis of gene expression related to TNF and TLR signaling pathways revealed higher expression levels in OLP patients, indicating uncontrolled inflammatory responses. The association between uncontrolled inflammation in OLP and aberrant regulation of TNF and TLR signaling pathways has been extensively discussed.[32,33,44,47] However, specific signaling pathways within the systemic immune system and the involved immune cell types remain unclear. In our study, subsequent investigation into cell-cell communication via LR interactions identified NK cells as significant contributors to TNF signaling activation in OLP patients, further implicating their role in driving inflammation and immune dysregulation.

PTGDS is known to play a critical role in regulating inflammation in astrocytes in Parkinson's disease, and it has also been recently associated with periodontitis, a chronic inflammatory condition.[48,49] In our study, *PTGDS* emerged as a potential diagnostic marker for OLP, with its upregulation observed in NK cells. This finding was further supported by elevated *PTGDS* expression in plasma samples, as confirmed by ELISA, and validated in the HRA002370 dataset. The consistent elevation across multiple platforms underscores its pivotal role in the immune dysregulation associated with OLP. These results suggest that *PTGDS* may not only serve as a diagnostic biomarker but also as a potential therapeutic target, offering new avenues for the treatment of OLP by modulating inflammatory pathways through *PTGDS* regulation. Further investigation into its specific functions within NK cells and its broader impact on the immune system in OLP is warranted to fully understand its clinical utility. Additionally, analysis of T cell subsets revealed an increased apoptosis and migration score, as well as a decreased immune tolerance score in OLP patients, indicative of systemic immune dysregulation and autoimmune features associated with the disease.[39,40] *CXCR4* has been reported to exhibit high expression in OLP patients, indicating its potential as a therapeutic target. However, the mechanism by which *CXCR4* governs the pathophysiological processes of OLP is not clearly understood.[30,50,51] In our study, we confirmed a correlation between *CXCR4* and *TSC22D3* expression. Interestingly, we identified a novel OLP-specific cluster of *CXCR4*^{high}-*TSC22D3*^{high} CD4 cytotoxic T cells in PBMCs, which was further validated by confirming its presence in the HRA002370 dataset. *CXCR4*^{high}-*TSC22D3*^{high} CD4 CTLs exhibited higher cytotoxicity compared to *CXCR4*^{low}-*TSC22D3*^{low} CD4 CTLs. *TSC22D3* is one of the glucocorticoid-induced genes and plays an important regulatory role in immune suppression and cell proliferation. *TSC22D3* participates in cellular responses to corticosteroid and glucocorticoid stimuli, which endogenous glucocorticoid signaling can influence, leading to T cell differentiation from a naive to a dysfunctional state. Previous research has suggested a regulatory cascade from glucocorticoid stimulation to the dysfunctional state mediated by *TSC22D3*. Additionally, it has been emphasized that stress-induced glucocorticoid surge and upregulation of *TSC22D3* can neutralize therapy-induced anti-cancer immune surveillance and impair anti-tumor

immunity by activating IFN-γ T cell activity. Notably, one critical regulator, *TSC22D3*, has frequently been identified in the state transitions from the intermediate state to the pre-dysfunction and dysfunction state of CD8 T cells, exerting diverse roles in each state transition through rewiring of regulatory interactions. It has been reported that *TSC22D3* is also highly expressed in CD4 T cells. However, the precise function of *TSC22D3* in CD4 T cells has not been elucidated.[52–55] Our results suggest that the *CXCR4*^{high}-*TSC22D3*^{high} cluster in CD4 CTLs may contribute to the cytotoxic mechanism and uncontrolled inflammatory response in the systemic immunity of OLP. This finding further elucidates the heterogeneity of T cell responses in OLP and underscores the importance of understanding transcriptional features in disease pathogenesis.

Our finding highlights distinct microenvironmental differences between OLP and LP, demonstrating that OLP is primarily driven by *TNF*-mediated inflammation, while LP exhibits enhanced VEGF signaling and vascular remodeling. These findings provide new insights into the differential pathophysiology of these two conditions and suggest potential mechanisms underlying their progression.

TNF, a key pro-inflammatory cytokine central to chronic inflammation through its promotion of immune cell activation, cytokine secretion, and tissue damage, may be further amplified by an imbalanced oral microbiota that has been proposed to induce Th17-mediated chronic inflammation and exacerbate tissue damage via upregulation of IL-6, IL-1β, and TGF-β, thereby promoting TNF signaling.[56–58] The strong *TNF–TNFRSF1B* interaction in OLP suggests a unique inflammatory signaling mechanism that may intensify immune activation and tissue damage, extending beyond the typical effects of *TNF* alone. While increased *TNF* expression in OLP is well established, our findings highlight *TNFRSF1B* as a key mediator of sustained inflammation, potentially amplifying keratinocyte apoptosis, epithelial barrier disruption, and prolonged immune infiltration. Given that *TNFRSF1B* preferentially promotes *TNF*-induced cell survival and immune regulation, its heightened activation in OLP may contribute to chronic inflammation and tissue remodeling unique to this condition.[59]

Beyond chronic inflammation, OLP is recognized as a potentially malignant disorder with an increased risk of oral squamous cell carcinoma (OSCC). Patients with OLP have been reported to have a significantly higher risk of developing tongue cancer and other forms of oral cancer compared to the general population.[60] This malignant potential is thought to be linked to persistent *TNF*-driven inflammation, oxidative stress, and chronic epithelial damage, which can create a microenvironment favorable for carcinogenesis.[61] These clinical implications highlight the importance of early detection and management of chronic inflammation in OLP to mitigate cancer risk.

In contrast, LP displayed a more interactive and pro-angiogenic microenvironment, with VEGF signaling being significantly stronger than in OLP. VEGF is a key regulator of angiogenesis, promoting endothelial cell proliferation and vascular remodeling.[62,63] The enhanced VEGF-mediated intercellular communication observed in LP, particularly among endothelial and stromal cells, suggests active tissue remodeling and vascularization. This aligns with previous studies showing increased VEGF expression in LP, which correlates with microvascular expansion and tissue remodeling.[64] These findings indicate that LP is regulated by a dynamic pro-angiogenic response, distinguishing it from the inflammatory pathology of OLP.

Previous studies have reported that keratinocyte proliferation in OLP is positively correlated with increased dermal microvascular density within the lesion.[65] Our results revealed that while *HIF1A*, a key hypoxia-related gene, was upregulated in OLP, VEGF LR interactions remained notably weak. *HIF1A* is known to induce VEGF expression under hypoxic conditions,[66] yet our findings suggest that OLP fails to translate this hypoxia signaling into effective VEGF-driven angiogenesis. One possible explanation is that the imbalance between *TNF*-driven inflammation and VEGF signaling in OLP may contribute to impaired vascular responses. Prior studies have shown that persistent inflammation can impair endothelial cell function and disrupt angiogenic signaling, leading to a dysregulated microenvironment.[67] Our findings further reinforce previous reports showing that VEGF expression is significantly lower in OLP compared to controls, whereas *HIF1A* expression is elevated.[68] However, our study uniquely demonstrates that this dysregulated hypoxia response is a distinct feature of OLP when compared to LP, which exhibits a more angiogenically active microenvironment. Unlike LP, where VEGF signaling drives vascular remodeling, OLP exhibits a disrupted hypoxia-angiogenesis axis with upregulated *HIF1A* but weak VEGF LR interactions. This distinction suggests that OLP is characterized by a hypoxia-driven inflammatory state rather than a pro-angiogenic response, further contributing to its

chronic disease progression and impaired tissue remodeling. This imbalanced hypoxia-VEGF signaling in OLP, which contrasts with the angiogenic signature of LP, may be a key factor driving sustained inflammation, prolonged immune activation, and delayed tissue healing in OLP lesions. These findings have important clinical implications. The strong *TNF–TNFRSF1B* interaction in OLP suggests *TNF*-targeted therapies may help mitigate chronic inflammation and tissue damage. The disrupted hypoxia-VEGF axis highlights the need for alternative approaches to restore vascular homeostasis and prevent disease progression. Additionally, given the increased risk of OSCC in OLP patients, regular monitoring and early intervention strategies are essential.[60]

This study has several limitations. An established animal model could not be utilized due to the unclear pathogenesis of OLP, limiting the ability to experimentally validate disease mechanisms. Additionally, the relatively small sample size may affect the generalizability of our findings. Despite these limitations, our study provides important insights into the distinct inflammatory and vascular differences between OLP and LP by evaluating systemic chronic inflammation at both the single-cell and protein levels. These findings identify potential diagnostic and therapeutic targets, laying the groundwork for future investigations.

Conclusions

Our study provides a comprehensive characterization of the immune landscape in OLP, offering critical insights into potential therapeutic targets and emphasizing key distinctions between OLP and LP. The distinct immune and signaling profiles observed in OLP suggest key molecular targets that may guide future intervention strategies. However, further functional validation of these biomarkers is necessary to confirm their clinical relevance. Longitudinal studies tracking immune responses in OLP and comparative analyses with LP will be essential for refining personalized treatment approaches and improving patient outcomes.

Data Sharing Statement

The datasets generated and analyzed during the current study are available in the Mendeley Data repository, at DOI: 10.17632/dzszp4pbc7.2.

Ethics Approval

This study was conducted in accordance with the tenets of Declaration of Helsinki after obtaining approval from the Institutional Review Board of Pusan National University Dental Hospital (IRB No. PNUDH-2021-12-027). Informed consent was obtained from all patients for being included in the study.

Author Contributions

All authors made a significant contribution to the work reported, whether that is in the conception, study design, execution, acquisition of data, analysis and interpretation, or in all these areas; took part in drafting, revising or critically reviewing the article; gave final approval of the version to be published; have agreed on the journal to which the article has been submitted; and agree to be accountable for all aspects of the work.

Funding

This work was supported by the Basic Science Research Program through the National Research Foundation of Korea (NRF), funded by the Ministry of Science and ICT (No. RS-2023-00209335). This work was also supported by the Medical Research Center Program (NRF-2018R1A5A2023879) through the National Research Foundation of Korea.

Disclosure

The authors report no conflicts of interest in this work.

References

1. González-Moles MÁ, Ruiz-Avila I, Gonzalez-Ruiz L, Ayen A, Gil-Montoya JA, Ramos-Garcia P. Malignant transformation risk of oral lichen planus: a systematic review and comprehensive meta-analysis. *Oral Oncology*. 2019;96:121–130. doi:10.1016/j.oraloncology.2019.07.012

2. González-Moles MÁ, Warnakulasuriya S, González-Ruiz I, et al. Worldwide prevalence of oral lichen planus: a systematic review and meta-analysis. *Oral Diseases*. 2021;27(4):813–828. doi:10.1111/odi.13323
3. Bombeccari GP, Guzzi G, Tettamanti M, et al. Oral lichen planus and malignant transformation: a longitudinal cohort study. *Oral Surgery, Oral Medicine, Oral Pathology, Oral Radiology, and Endodontology*. 2011;112(3):328–334. doi:10.1016/j.tripleo.2011.04.009
4. Torrente Castells E, Barbosa de Figueiredo RP, Berini Aytés L, Gay Escoda C. Clinical features of oral lichen planus. A retrospective study of 65 cases. *Medicina Oral, Patología Oral y Cirugía Bucal*. 2010;15(5):685–690. doi:10.4317/medoral.15.e685
5. Nielsen F, Mikkelsen BB, Nielsen JB, Andersen HR, Grandjean P. Plasma malondialdehyde as biomarker for oxidative stress: reference interval and effects of life-style factors. *Clinical Chemistry*. 1997;43(7):1209–1214. doi:10.1093/clinchem/43.7.1209
6. DeAngelis LM, Cirillo N, McCullough MJ. The immunopathogenesis of oral lichen planus—Is there a role for mucosal associated invariant T cells? *Journal of Oral Pathology & Medicine*. 2019;48(7):552–559. doi:10.1111/jop.12898
7. Khan A, Farah CS, Savage NW, Walsh LJ, Harbrow DJ, Sugerman PB. Th1 cytokines in oral lichen planus. *Journal of Oral Pathology & Medicine*. 2003;32(2):77–83. doi:10.1034/j.1600-0714.2003.00077.x
8. Lu R, Zhou G, Du G, Xu X, Yang J, Hu J. Expression of T-bet and GATA-3 in peripheral blood mononuclear cells of patients with oral lichen planus. *Archives of Oral Biology*. 2011;56(5):499–505. doi:10.1016/j.archoralbio.2010.11.006
9. El-Howati A, Thornhill MH, Colley HE, Murdoch C. Immune mechanisms in oral lichen planus. *Oral Diseases*. 2023;29(4):1400–1415. doi:10.1111/odi.14142
10. Sugerman P, Savage N, Walsh L, et al. The pathogenesis of oral lichen planus. *Critical Reviews in Oral Biology & Medicine*. 2002;13(4):350–365. doi:10.1177/154411130201300405
11. Deng X, Wang Y, Jiang L, Li J, Chen Q. Updates on immunological mechanistic insights and targeting of the oral lichen planus microenvironment. *Frontiers in Immunology*. 2023;13:1023213. doi:10.3389/fimmu.2022.1023213
12. Lee H, Joo J-Y, Sohn DH, et al. Single-cell RNA sequencing reveals rebalancing of immunological response in patients with periodontitis after non-surgical periodontal therapy. *Journal of Translational Medicine*. 2022;20(1):504. doi:10.1186/s12967-022-03702-2
13. Lee H, Joo JY, Song JM, Kim HJ, Kim YH, Park HR. Immunological link between periodontitis and type 2 diabetes deciphered by single-cell RNA analysis. *Clinical and Translational Medicine*. 2023;13(12):e1503. doi:10.1002/ctm2.1503
14. Lee H, Park S, Yun JH, et al. Deciphering head and neck cancer microenvironment: single-cell and spatial transcriptomics reveals human papillomavirus-associated differences. *Journal of Medical Virology*. 2024;96(1):e29386. doi:10.1002/jmv.29386
15. Wu X, Liu Y, Jin S, et al. Single-cell sequencing of immune cells from anticitrullinated peptide antibody positive and negative rheumatoid arthritis. *Nat Commun*. 2021;12(1):4977. doi:10.1038/s41467-021-25246-7
16. Nehar-Belaid D, Hong S, Marches R, et al. Mapping systemic lupus erythematosus heterogeneity at the single-cell level. *Nat Immunol*. 2020;21(9):1094–1106. doi:10.1038/s41590-020-0743-0
17. Jovic D, Liang X, Zeng H, Lin L, Xu F, Luo Y. Single-cell RNA sequencing technologies and applications: a brief overview. *Clin Transl Med*. 2022;12(3):e694. doi:10.1002/ctm2.694
18. Eberwine J, Sul JY, Bartfai T, Kim J. The promise of single-cell sequencing. *Nat Methods*. 2014;11(1):25–27. doi:10.1038/nmeth.2769
19. Li X, Wang CY. From bulk, single-cell to spatial RNA sequencing. *Int J Oral Sci*. 2021;13(1):36. doi:10.1038/s41368-021-00146-0
20. Weston G, Payette M. Update on lichen planus and its clinical variants. *International Journal of Women's Dermatology*. 2015;1(3):140–149. doi:10.1016/j.ijwd.2015.04.001
21. Van der Meij E, Van der Waal I. Lack of clinicopathologic correlation in the diagnosis of oral lichen planus based on the presently available diagnostic criteria and suggestions for modifications. *Journal of Oral Pathology & Medicine*. 2003;32(9):507–512. doi:10.1034/j.1600-0714.2003.00125.x
22. Andrews S. Babraham bioinformatics-FastQC a quality control tool for high throughput sequence data. 2010. Available from: https://www.bioinformatics.babraham.ac.uk/projects/fastqc. Accessed Mar 10, 2025.
23. Cunningham F, Allen JE, Allen J, et al. Ensembl 2022. *Nucleic Acids Research*. 2022;50(D1):D988–D995. doi:10.1093/nar/gkab1049
24. Hao Y, Hao S, Andersen-Nissen E, et al. Integrated analysis of multimodal single-cell data. *Cell*. 2021;184(13):3573–3587.e29. doi:10.1016/j.cell.2021.04.048
25. Aran D, Looney AP, Liu L, et al. Reference-based analysis of lung single-cell sequencing reveals a transitional profibrotic macrophage. *Nature Immunology*. 2019;20(2):163–172. doi:10.1038/s41590-018-0276-y
26. Phipson B, Sim CB, Porrello ER, Hewitt AW, Powell J, Oshlack A. propeller: testing for differences in cell type proportions in single cell data. *Bioinformatics*. 2022;38(20):4720–4726. doi:10.1093/bioinformatics/btac582
27. Jin S, Guerrero-Juarez CF, Zhang L, et al. Inference and analysis of cell-cell communication using CellChat. *Nature Communications*. 2021;12(1):1088. doi:10.1038/s41467-021-21246-9
28. Andreatta M, Carmona SJ. UCell: robust and scalable single-cell gene signature scoring. *Computational and Structural Biotechnology Journal*. 2021;19:3796–3798. doi:10.1016/j.csbj.2021.06.043
29. Zhang J-Y, Wang X-M, Xing X, et al. Single-cell landscape of immunological responses in patients with COVID-19. *Nature Immunology*. 2020;21(9):1107–1118. doi:10.1038/s41590-020-0762-x
30. Li Q, Wang F, Kuang W, et al. Single-cell immune profiling reveals immune responses in oral lichen planus. *Frontiers in Immunology*. 2023;14:1182732. doi:10.3389/fimmu.2023.1182732
31. Kersh AE, Sati S, Huang J, Murphy C, Ahart O, Leung TH. CXCL9, CXCL10, and CCL19 synergistically recruit T lymphocytes to skin in lichen planus. *JCI Insight*. 2024;9(20):e179899. doi:10.1172/jci.insight.179899
32. Lu R, Zhang J, Sun W, Du G, Zhou G. Inflammation-related cytokines in oral lichen planus: an overview. *Journal of Oral Pathology & Medicine*. 2015;44(1):1–14. doi:10.1111/jop.12142
33. Wang Y, Zhang H, Du G, et al. Total glucosides of paeony (TGP) inhibits the production of inflammatory cytokines in oral lichen planus by suppressing the NF-κB signaling pathway. *International Immunopharmacology*. 2016;36:67–72. doi:10.1016/j.intimp.2016.04.010
34. Nagata A, Suzuki Y, Igarashi M, et al. Human brain prostaglandin D synthase has been evolutionarily differentiated from lipophilic-ligand carrier proteins. *Proceedings of the National Academy of Sciences*. 1991;88(9):4020–4024. doi:10.1073/pnas.88.9.4020

35. Nordkamp MJO, van Roon JA, Douwes M, de Ruiter T, Urbanus RT, Meyaard L. Enhanced secretion of leukocyte-associated immunoglobulin-like receptor 2 (LAIR-2) and soluble LAIR-1 in rheumatoid arthritis: LAIR-2 is a more efficient antagonist of the LAIR-1–collagen inhibitory interaction than is soluble LAIR-1. *Arthritis & Rheumatism*. 2011;63(12):3749–3757. doi:10.1002/art.30612
36. Lebbink RJ, Raynal N, de Ruiter T, Bihan DG, Farndale RW, Meyaard L. Identification of multiple potent binding sites for human leukocyte associated Ig-like receptor LAIR on collagens II and III. *Matrix Biology*. 2009;28(4):202–210. doi:10.1016/j.matbio.2009.03.005
37. Meyaard L, Adema GJ, Chang C, et al. LAIR-1, a novel inhibitory receptor expressed on human mononuclear leukocytes. *Immunity*. 1997;7 (2):283–290. doi:10.1016/S1074-7613(00)80530-0
38. Wang H, Zhang D, Han Q, et al. Role of distinct CD 4+ T helper subset in pathogenesis of oral lichen planus. *Journal of Oral Pathology & Medicine*. 2016;45(6):385–393. doi:10.1111/jop.12405
39. Wu P, Luo S, Zhou T, et al. Possible mechanisms involved in the cooccurrence of oral lichen planus and hashimoto's thyroiditis. *Mediators of Inflammation*. 2020;2020:1–9. doi:10.1155/2020/6309238
40. De Porras-Carrique T, Ramos-García P, Aguilar-Diosdado M, Warnakulasuriya S, MÁ G. Autoimmune disorders in oral lichen planus: a systematic review and meta-analysis. *Oral Diseases*. 2023;29(4):1382–1394. doi:10.1111/odi.14127
41. Roopashree M, Gondhalekar RV, Shashikanth M, George J, Thippeswamy S, Shukla A. Pathogenesis of oral lichen planus–a review. *Journal of Oral Pathology & Medicine*. 2010;39(10):729–734. doi:10.1111/j.1600-0714.2010.00946.x
42. Kurago ZB. Etiology and pathogenesis of oral lichen planus: an overview. *Oral Surgery, Oral Medicine, Oral Pathology and Oral Radiology*. 2016;122(1):72–80. doi:10.1016/j.oooo.2016.03.011
43. Weber B, Schlapbach C, Stuck M, et al. Distinct interferon-gamma and interleukin-9 expression in cutaneous and oral lichen planus. *Journal of the European Academy of Dermatology and Venereology*. 2017;31(5):880–886. doi:10.1111/jdv.13989
44. Miyahara Y, Chen H, Moriyama M, et al. Toll-like receptor 9-positive plasmacytoid dendritic cells promote Th17 immune responses in oral lichen planus stimulated by epithelium-derived cathepsin K. *Scientific Reports*. 2023;13(1):19320. doi:10.1038/s41598-023-46090-3
45. Afzali S, Mohammadisoleimani E, Mansoori Y, et al. The potential roles of Th17 cells in the pathogenesis of oral lichen planus. *Inflammation Research*. 2023;72(7):1513–1524. doi:10.1007/s00011-023-01763-7
46. Carrozzo M. Understanding the pathobiology of oral lichen planus. *Current Oral Health Reports*. 2014;1(3):173–179. doi:10.1007/s40496-014-0022-y
47. Du GH, Qin XP, Li Q, Zhou YM, Shen XM, Tang GY. The high expression level of programmed death-1 ligand 2 in oral lichen planus and the possible costimulatory effect on human T cells. *Journal of Oral Pathology & Medicine*. 2011;40(7):525–532. doi:10.1111/j.1600-0714.2011.01035.x
48. Choi D-J, An J, Jou I, Park SM, Joe E-H. A Parkinson's disease gene, DJ-1, regulates anti-inflammatory roles of astrocytes through prostaglandin D2 synthase expression. *Neurobiology of Disease*. 2019;127:482–491. doi:10.1016/j.nbd.2019.04.003
49. Suzuki A, Ji G, Numabe Y, et al. Single nucleotide polymorphisms associated with aggressive periodontitis and severe chronic periodontitis in Japanese. *Biochemical and Biophysical Research Communications*. 2004;317(3):887–892. doi:10.1016/j.bbrc.2004.03.126
50. Ichimura M, Hiratsuka K, Ogura N, et al. Expression profile of chemokines and chemokine receptors in epithelial cell layers of oral lichen planus. *Journal of Oral Pathology & Medicine*. 2006;35(3):167–174. doi:10.1111/j.1600-0714.2006.00402.x
51. Rivera C, Crisóstomo MF, Peña C, González-Díaz P, González-Arriagada WA. Oral lichen planus interactome reveals CXCR4 and CXCL12 as candidate therapeutic targets. *Scientific Reports*. 2020;10(1):5454. doi:10.1038/s41598-020-62258-7
52. Yan M, Hu J, Yuan H, et al. Dynamic regulatory networks of T cell trajectory dissect transcriptional control of T cell state transition. *Molecular Therapy-Nucleic Acids*. 2021;26:1115–1129. doi:10.1016/j.omtn.2021.10.011
53. Li Y, Huang H, Zhu Z, Chen S, Liang Y, Shu L. TSC22D3 as an immune-related prognostic biomarker for acute myeloid leukemia. *Iscience*. 2023;26(8):1.
54. Yang H, Xia L, Chen J, et al. Stress–glucocorticoid–TSC22D3 axis compromises therapy-induced antitumor immunity. *Nature Medicine*. 2019;25 (9):1428–1441. doi:10.1038/s41591-019-0566-4
55. Li Y, Zhu Z, Chen S, et al. Identification of TSC22D3 As a Novel Immune-Related Prognostic Biomarker of Acute Myeloid Leukemia. *Blood*. 2022;140(Supplement 1):11799–11800. doi:10.1182/blood-2022-168786
56. Aggarwal BB, Gupta SC, Kim JH. Historical perspectives on tumor necrosis factor and its superfamily: 25 years later, a golden journey. *Blood, the Journal of the American Society of Hematology*. 2012;119(3):651–665.
57. Balkwill F. Tumour necrosis factor and cancer. *Nature Reviews Cancer*. 2009;9(5):361–371. doi:10.1038/nrc2628
58. Larsen JM. The immune response to Prevotella bacteria in chronic inflammatory disease. *Immunology*. 2017;151(4):363–374. doi:10.1111/imm.12760
59. Gupta S, Jawanda MK. Oral lichen planus: an update on etiology, pathogenesis, clinical presentation, diagnosis and management. *Indian Journal of Dermatology*. 2015;60(3):222–229. doi:10.4103/0019-5154.156315
60. Gandolfo S, Richiardi L, Carrozzo M, et al. Risk of oral squamous cell carcinoma in 402 patients with oral lichen planus: a follow-up study in an Italian population. *Oral Oncology*. 2004;40(1):77–83. doi:10.1016/S1368-8375(03)00139-8
61. Karin M, Greten FR. NF-κB: linking inflammation and immunity to cancer development and progression. *Nature Reviews immunology*. 2005;5 (10):749–759. doi:10.1038/nri1703
62. Byrne AM, Bouchier-Hayes DJ, Harmey JH. Angiogenic and cell survival functions of vascular endothelial growth factor (VEGF). *Journal of Cellular and Molecular Medicine*. 2005;9(4):777–794. doi:10.1111/j.1582-4934.2005.tb00379.x
63. Veikkola T, Karkkainen M, Claesson-Welsh L, Alitalo K. Regulation of angiogenesis via vascular endothelial growth factor receptors. *Cancer Research*. 2000;60(2):203–212.
64. Výbohová D, Mellová Y, Adamicová K, Adamkov M, Hešková G. Quantitative comparison of angiogenesis and lymphangiogenesis in cutaneous lichen planus and psoriasis: immunohistochemical assessment. *Acta Histochemica*. 2015;117(1):20–28. doi:10.1016/j.acthis.2014.10.008
65. Alsohaimi A. The pathogenic role of vascular endothelial growth factor (VEGF) in skin diseases. *Adv Med Med Res*. 2019;2(1):27–37. doi:10.31377/ammr.v2i1.634
66. Semenza GL. Hypoxia-inducible factors in physiology and medicine. *Cell*. 2012;148(3):399–408. doi:10.1016/j.cell.2012.01.021
67. Carmeliet P, Jain RK. Molecular mechanisms and clinical applications of angiogenesis. *Nature*. 2011;473(7347):298–307. doi:10.1038/nature10144
68. Ding M, Xu J, Fan Y. Altered expression of mRNA for HIF-1α and its target genes RTP801and VEGF in patients with oral lichen planus. *Oral Diseases*. 2010;16(3):299–304. doi:10.1111/j.1601-0825.2009.01645.x